Tianjin Daxue Xuebao (Ziran Kexue yu Gongcheng Jishu Ban)/
Journal of Tianjin University Science and Technology
ISSN (Online):0493-2137
E-Publication: Online Open Access
Vol: 59 Issue: 02:2026
DOI: 10.5281/zenodo.18617972

PROTECTIVE EFFECT OF QUERCETIN NANOEMULSION ON METHOTREXATE-INDUCED LINGUAL MUCOSITIS IN RATS

MENNA REDA FARRAG
Demonstrator in Oral and Maxillofacial Pathology Department, Faculty of Dentistry, Suez Canal University, Egypt. Email: menna_reda@dent.suez.edu.eg

SARA A. SWIDAN
Lecturer of Oral and Maxillofacial Pathology Department, Faculty of Dentistry, Suez Canal University, Egypt. Email: sara_sowidan@dent.suez.edu.eg

MERHAN NABIH ELMANSY
Assistant Professor, Oral and Maxillofacial Pathology Department, Faculty of Dentistry, Suez Canal University, Egypt. Email: merhan_elmansy@dent.suez.edu.eg

Abstract

Background: Oral mucositis (OM) is a common debilitating side effect induced by methotrexate (MTX). Quercetin (QRC) is a natural flavonoid with anti-inflammatory and antioxidant properties. Formulating QRC in nanoemulsion (QRC-NE) may enhance its biological effects and therapeutic potential. **Aim:** This study evaluated the histopathological and immunohistochemical effects of QRC-NE on MTX-induced lingual mucositis in albino rats. **Material and Methods:** Fifty animals were randomly divided into five groups: Negative control (healthy), MTX-treated (a single i.p. 20 mg/kg on day 11), QRC-treated (50 mg/kg orally, 16 days), QRC+MTX and QRC-NE+MTX (QRC 50 mg/kg and QRC-NE 12.5 mg/kg, respectively, orally as a prophylactic to OM, 16 days + MTX a single i.p. 20 mg/kg on day 11). Rats were euthanized on day 17. The anterior two-thirds of tongue specimens were processed for histological assessment by H&E and Masson Trichrome staining, and Caspase-3 IHC expression. Data were analyzed using the one-way ANOVA and Bonferroni post-hoc tests. **Results:** MTX group revealed marked histological destruction in the lingual mucosa with reduced collagen density and strong caspase-3 expression compared to the negative control ($p \leq 0.05$). QRC-NE treatment showed significantly preserved mucosal architecture, increased collagen density, and exhibited mild caspase-3 expression compared to MTX ($p \leq 0.05$). **Conclusions**: QRC-NE has a modulatory effect on MTX-induced lingual mucositis, suggesting a potential role for nano-based QRC administration in alleviating oral mucosal injury.

Keywords: Caspase-3; Methotrexate; Nanoemulsion; Oral mucositis; Quercetin.

1. INTRODUCTION

Methotrexate (MTX) is an antimetabolite drug and chemotherapeutic agent that has been widely used in the treatment of several malignant conditions, as well as other diseases such as rheumatoid arthritis, and ulcerative colitis [1]. MTX is considered a dihydrofolate reductase enzyme inhibitor (DHFR) that stops cell division and promotes apoptosis as it blocks DNA synthesis [2]. Common side effects associated with MTX treatment involve multi-organ toxicities, immunosuppression, inflammatory or lymphoproliferative disorders, and major adverse effects on the salivary glands [3].

Oral mucositis (OM) is a disabling adverse effect associated with MTX treatment that causes feeding challenges, raises the risk of infection, and postpones therapy [4]. The pathophysiology of OM consists of five phases: initiation, upregulation with messenger

Tianjin Daxue Xuebao (Ziran Kexue yu Gongcheng Jishu Ban)/
Journal of Tianjin University Science and Technology
ISSN (Online):0493-2137
E-Publication: Online Open Access
Vol: 59 Issue: 02:2026
DOI: 10.5281/zenodo.18617972

generation, signalling and amplification, ulceration and inflammation, and finally, healing [5]. Quercetin (QRC) is a naturally occurring flavonoid found in tea, apples, red wine, onions, broccoli, kale, oranges, and blueberries [6]. QRC has been proven to have antioxidant, cardiovascular protective, anticancer, antitumor, anti-inflammatory, anti-diabetic, and immunomodulatory activities [7]. Despite its advantages, QRC is highly lipophilic with low water solubility and bioavailability, limiting its potential therapeutic application due to poor intestinal absorption [8].

Drug delivery through nanoformulation, such as nanoemulsion (NE), improves the drug's solubility, absorption, and intestinal bioavailability. Moreover, it stops the drug molecules from premature breaking down before it reaches the lesion, increases the drug's bioavailability and extends its circulation time [9].

The process of apoptosis is extremely complicated and involves a series of molecular reactions. Two major general pathways regulate apoptosis: the intrinsic (mitochondrial) and extrinsic (death receptor) pathways [10]. Both pathways converge at the execution pathway to start the apoptotic process. Execution caspases such as caspases -3, -6, and -7 activate cytoplasmic endonuclease and degrade the cytoskeleton proteins, cell cycle, and signalling pathways, which together contribute to the morphological changes in the programmed cell death [11].

This study was designed to study the possible protective effect of QRC-NE supplementation through evaluation of the histopathological changes and immunohistochemical expression of caspase-3 in MTX-induced lingual mucositis in albino rats.

2. MATERIAL AND METHODS

2.1 Materials:

Methotrexate (MTX) 50 mg / 2 ml of solution was purchased from Hikma Specialized Pharmaceuticals, Egypt. QRC was purchased from Sigma Chemical Company, USA. Cat. No. 6151253]. QRC powder (3.20 g) was dissolved in distilled water (320 ml) to ensure that each milli-Liter of the solution had 10 mg of QRC [12].

2.2 Preparation for Quercetin nanoemulsion (QRC-NE):

The QRC-NE was prepared using the ultrasonication method [13]. 800 mg of pure QRC was dissolved in Tween 80 and caprylic triglyceride using a magnetic stirrer for 1 hour at 65 °C. Then, the mixture was subjected to a high-speed homogenizer (Ultra-Turrax T-25, Janhke & Kunkel Gmbh and Co KG, Staufen, Germany) for 4 minutes at 12,000 rpm. The primary emulsion mixture was mixed with pure water and gently stirred for 3 hours to prepare the NE.

2.3 Characterization of QRC-NE:

The synthesis of QRC-NE was studied using Fourier transform infrared spectroscopy (FTIR) (Bruker Corp., Massachusetts, USA). To characterize the morphology of the prepared particles, transmission electron microscope (TEM) was used (JEOL JEM-2100

Tianjin Daxue Xuebao (Ziran Kexue yu Gongcheng Jishu Ban)/
Journal of Tianjin University Science and Technology
ISSN (Online):0493-2137
E-Publication: Online Open Access
Vol: 59 Issue: 02:2026
DOI: 10.5281/zenodo.18617972

Electron Microscope). The Dynamic light scattering (DLS) was used to study the hydrodynamic particle size, polydispersity index (PDI), and zeta potential measurements at room temperature by Malvern Zeta sizer Nano ZS90.

2.4 Sample size calculation:

The sample size for this study was calculated according to **Charan and Biswas (2013)** [14] using the following equation:

$$N = \frac{(z\alpha)2\ x\ (SD)2}{(d)2}$$

N = Total sample size

Z_α= Is Standard normal variate and its equal 1.96 at P< 0.05

SD = Standard diversion of variable

d = Absolute error or precision

Zα	SD	D
1.96	7.20	2

Total sample size N= $\frac{(1.96)2\ x\ (7.20)2}{(2)2}$ = 49.787≈50 samples

The total sample size calculations revealed that a sample size should be **5**0

2.5 Experimental design:

Fifty male albino rats (6 to 8 weeks), 150-200 grams, were kept in the Animal House, Faculty of Dentistry, Suez Canal University (Ismailia, Egypt). They were housed in a well-ventilated room with controlled temperature, 50-70% humidity, and a 12-hour day/night cycle. They were given a standard diet & tap water. This study was approved by the Research Ethical Committee (REC), Faculty of Dentistry, Suez Canal University, with approval No. (874/2024) and all procedures were performed in accordance with the **ARRIVE guidelines**.

Animals were randomly assigned to five experimental groups (n= 10 per group) using a computer- generated sequence as follows: Group 1 (negative control) are healthy received no treatment. Group 2 (MTX-treated group) served as a positive control and received MTX (20 mg/kg) as a single intraperitoneal injection (I.P.) on day 11 [15]. Group 3 (QRC-treated group) served as a self-control group that received only QRC (50 mg/kg) daily by oral gavage from day 1 to day 16 [15].

Group 4 (MTX+QRC) and Group 5 (QRC-NE+MTX) received QRC (50 mg/kg) and QRC-NE 12.5 mg/kg [16], respectively. The drugs were given as prophylaxis to OM daily by oral gavage from day 1 to day 16, and MTX (20 mg/kg) was administered as a single I.P. on day 11. The animals were euthanized by Carbon dioxide (CO2) inhalation on day 17.

The anterior two-thirds of the tongue tissues were dissected and preserved for 24 hours in a 10% neutral buffered formalin solution. Histological and immunohistochemical evaluations were conducted blinded to group allocation to ensure unbiased assessment.

Tianjin Daxue Xuebao (Ziran Kexue yu Gongcheng Jishu Ban)/
Journal of Tianjin University Science and Technology
ISSN (Online):0493-2137
E-Publication: Online Open Access
Vol: 59 Issue: 02:2026
DOI: 10.5281/zenodo.18617972

2.6 Clinical assessment

All rats were weighed at the beginning and end of the experiment. The animals were regularly examined for any clinically evident hair loss. According to the OM scoring system scale, which includes the following levels [17].

Grade 0: normal, Grade 1: slight red, Grade 2: severe redness, Grade 3: focal desquamation, Grade 4: exudation covering half of the mucosa, Grade 5: complete ulceration.

2.7 Histological and immunohistochemical analysis:

The samples were subsequently processed, paraffin-embedded, sectioned into 5 μm pieces, mounted, and stained with hematoxylin and eosin for light microscopic analysis to assess the overall histopathological alterations in the filiform papillae's length & width, the fungiform papillae's width, the epithelial thickness of the ventral surface, the width of blood vessels, the cystic degeneration of the Weber salivary gland (WG), and Von Ebner gland (VG).

Masson Trichrome stain was used to study the density of collagen. Organized collagen fibres had a deep blue colour, while disorganized collagen fibres had a light blue colour.

Five μm-thick sections were cut and mounted on positively charged slides for caspase-3 staining using a rabbit polyclonal antibody to Caspase-3 (R&D Systems, Cat. No. AF-835) according to the manufacturer's instructions. Positive results were indicated by cytoplasmic brown staining with different intensities [18]. The slides were examined and photographed by E-330 Olympus digital camera.

2.8 Morphometric analysis:

Quantitative analysis was performed using an image analyser computer system (ImageJ / Fiji 1.46) to measure the different histological criteria. Digitizing the slides under 400X objective magnification enabled the measurement of the mean collagen density stained by Masson trichrome and counting the number of immune-positive cells (Caspase-3), as well as the number of remaining unstained ones. So, the fraction in five photograph fields was calculated.

2.9 Statistical Analysis:

The SPSS software for Windows version 26.0, GraphPad Prism, and Excel Microsoft was used to conduct statistical analysis of the data collected. Data were presented as mean ± standard deviation. One-way ANOVA and Tukey`s post hoc tests were used for multiple comparisons. Different letters meant significant difference between groups at P value ≤ 0.05.

Tianjin Daxue Xuebao (Ziran Kexue yu Gongcheng Jishu Ban)/
Journal of Tianjin University Science and Technology
ISSN (Online):0493-2137
E-Publication: Online Open Access
Vol: 59 Issue: 02:2026
DOI: 10.5281/zenodo.18617972

3. RESULTS:

3.1 Characterization of QRC-NE:

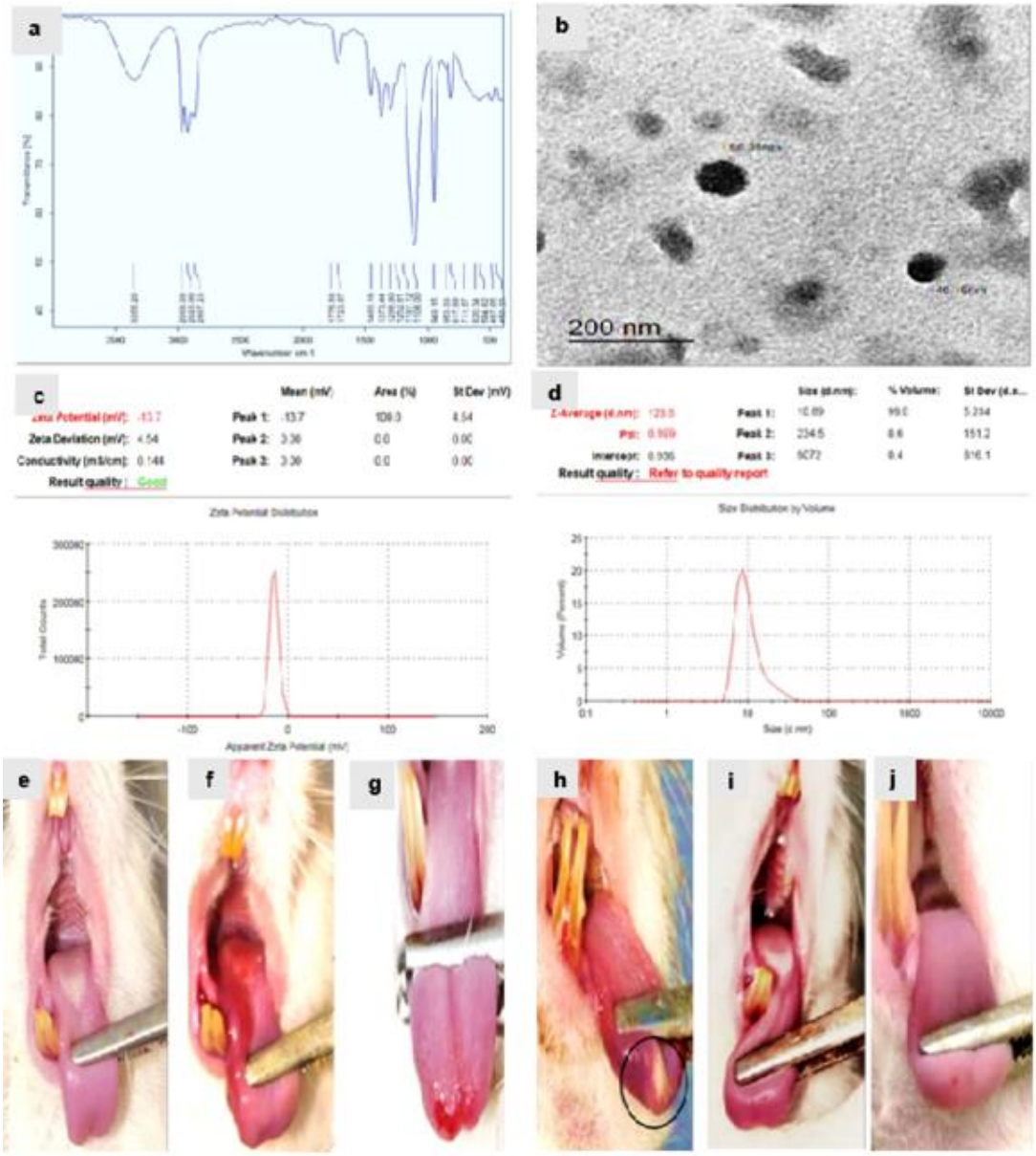

Fig. 1: (a-d) Results of QRC-NE characterization (a) FTIR spectra . (b) TEM image. (c) Zeta potential. (d) Particle size distribution curve. (e-j) Photographs of lingual mucosa (e) Normal mucosa in the negative control and QRC groups. (f-h) In MTX group (f) Severe redness. (g) Focal desquamation. (h) Ulcer (black circle). (i) Slight to severe redness in QRC+MTX group (j) Near normal to slight redness in QRC-NE+MTX

Tianjin Daxue Xuebao (Ziran Kexue yu Gongcheng Jishu Ban)/
Journal of Tianjin University Science and Technology
ISSN (Online):0493-2137
E-Publication: Online Open Access
Vol: 59 Issue: 02:2026
DOI: 10.5281/zenodo.18617972

The FTIR spectrum confirmed the formation of QRC-NE, where its characteristic bonds (Fig. 1a). The peak at 3355.26 cm−1 corresponded to the O-H stretch. The peaks at 2966.99, 2923.88, and 2867.23 cm−1 corresponded to the C-H stretch. The peaks at 1775.56 and 1723.97 cm−1 indicated C=O stretch, while the peaks at 1460 and 1373.44 cm−1 revealed C-H bending. The peaks at 1298.90 and 1252.81 cm−1 were C-O stretch, confirming the presence of tween. The TEM images of the prepared QRC-NE showed spherical particles with an average diameter of 46.16±20.19 nm, indicating a uniform stable NE (Fig. 1b).

The mean zeta potential for QRC-NE was found to be 13.7±4.54mV, indicating a moderate surface charge with limited stability (Fig. 1c). DLS showed the mean hydrodynamic particle size was 123.5±5.234 nm, and the polydispersity index (PdI) was found to be 0.599, indicating a heterogeneous size distribution (Fig. 1d).

The prepared QRC-NE formulation was used immediately in the present study, and therefore, no stability issues were observed during the experiments. Nevertheless, the relatively high PDI and moderate zeta potential suggest that further optimization may be needed to improve long-term uniformity and stability. Additionally, encapsulation efficiency, drug loading, and release kinetics were not evaluated, which should be addressed in future studies to fully confirm the formulation's reliability and efficacy.

3.2 Clinical findings:

There was a significant loss of body weight in MTX-treated group (165.4±3.0) in comparison to the negative control group and QRC group (211±7.3a & 202.2±6.5), respectively. There was a slight improvement in the general health of albino rats in QRC+MTX group (179.6±8.3), while a marked improvement was noticed in QRC-NE+MTX group (195.8±5.9) in comparison to the positive control group (165.4±3.0). All animals exhibited normal hair distribution, except for G2, which displayed moderate to severe hair loss, and G4 (QRC+MTX), which showed mild to moderate hair loss.

According to the OM scoring system scale, negative control and QRC groups showed normal lingual mucosa (grade 0). In MTX group, severe redness was observed in 50% (grade 2), focal desquamation in 10% (grade 3), exudation in 20% (grade 4), and complete ulceration in 20% of animals (grade 5).

Animals in G4 (QRC+MTX) showed slight red mucosa in 30 % (grade 1), while severe redness in 40% (grade 2), and focal desquamation in 30% (grade 3). Rats of G5 (QRC-NE+MTX) showed normal mucosa in 30% (grade 0), slightly red mucosa in 50% (grade 1), and severe redness in 20% (grade 2) (Fig.1e–j).

3.3 Histopathological assessment:

The negative control and QRC groups showed normal keratinized stratified squamous epithelium with sharp, conical filiform papillae with pointed tips. Their length ranged from 1093.30±47.32& 1036.93±18.88, and their width was 181.63±12.86 & 183.80±13.08 in both groups, respectively (Fig. 2a & 2g).

Tianjin Daxue Xuebao (Ziran Kexue yu Gongcheng Jishu Ban)/
Journal of Tianjin University Science and Technology
ISSN (Online):0493-2137
E-Publication: Online Open Access
Vol: 59 Issue: 02:2026
DOI: 10.5281/zenodo.18617972

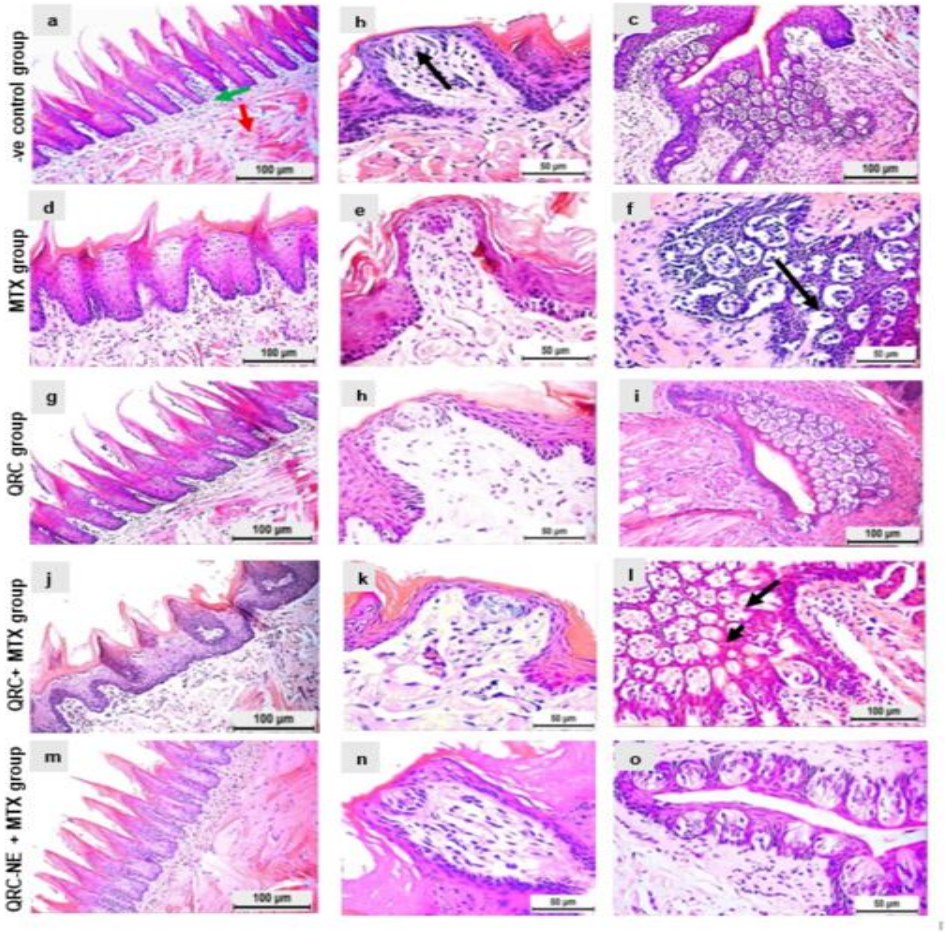

Fig. 2: Photomicrographs of lingual mucosa showing: (a-c) Negative control group (a) Sharp conical projections of filiform papillae with keratinized stratified squamous epithelium, and the underlying lamina propria and muscle bundles. (b) Normal taste bud of fungiform papillae. (c) Multiple taste buds of circumvallate papilla. (d-f) MTX group (d) Atrophic filiform papillae. (e) degenerated taste bud with marked inflammation. (f) degenerated taste buds of circumvallate papillae. (g-i) Normal histological features in QRC group. (j-l) QRC+MTX group (j) Atrophic filiform papillae. (k) Cytoplasmic vacuolization of taste bud. (l) some normal (green arrows) and degenerated buds (black arrows) of circumvallate papillae. (m-o) QRC-NE+MTX group (m) Normal filiform papillae. (n) Normal taste bud. (o) multiple taste buds. {lamina propria (green arrow), muscles (red arrow), and Taste bud (black arrows) [H&E-stained sections. Magnifications: a, c, d, g, i, j, l, & m: X20 / b, e, f, h, k, n, & o: X 40]

Fungiform papillae were few, with one taste bud on their upper surface. Their width was 468.53±9.52 and 511.69±10.90, respectively (Fig. 2b & 2h). Multiple taste buds of the circumvallate papillae were seen (Fig. 2c & 2i). The ventral surface showed normal epithelial thickness (490.64±14.35 & 490.32±11.10) (Fig. 3a & 3g). The underlying

Tianjin Daxue Xuebao (Ziran Kexue yu Gongcheng Jishu Ban)/
Journal of Tianjin University Science and Technology
ISSN (Online):0493-2137
E-Publication: Online Open Access
Vol: 59 Issue: 02:2026
DOI: 10.5281/zenodo.18617972

connective tissue (c.t.) appeared normal with minimal infiltration of inflammatory cells and no dilated blood vessels (102.03±9.29 & 113.09±14.12). Normal architecture of WG without any cystic degeneration (58.71±5.84 & 67.82±6.78) (Fig. 3b & 3h), and normal microscopic features of VG were observed (Fig. 3c & 3i). (Table 1).

Table 1: illustrating statistical significance of histomorphometrically data in different groups

	G1 (-ve control)	G2 (MTX group)	G3 (QRC group)	G4 (QRC+MTX)	G5 (QRC-NE+MTX)
Animal weight	211±7.3a	165.4±3.0b	202.2±6.5a	179.6±8.3b	195.8±5.9a
Filiform length	1093.30±47.32a	551.66±29.62c	1036.93±18.88a	797.99±13.35b	1054.87±10.38a
Filiform width	181.63±12.86c	289.63±8.99a	183.80±13.08c	221.92±10.45b	179.99±14.09c
Fungiform width	468.53±9.52a	336.22±11.29c	511.69±10.90a	380.75±13.70b	461.81±8.69a
Cystic space width	58.71±5.84c	386.37±11.53a	67.82±6.78c	137.74±9.52b	67.42±5.75c
Ventral thickness	490.64±14.35a	127.40±10.86c	490.32±11.10a	243.96±13.76b	474.31±12.72a
Blood vessel width	102.03±9.29c	783.43±22.83a	113.09±14.12c	571.35±10.85b	137.33±8.99c
Collagen density	62.12±5.86a	25.16±6.06c	58.00±4.64a	37.92±4.92b	57.43±8.11a
Caspase-3	12.59±0.77c	51.83±1.56a	13.32±0.97c	39.21±3.24b	23.77±1.45c
**, a,b,c; mean significant difference between groups using an independent T-test at P value ≤ 0.05					

In MTX group, filiform papillae revealed loss of their conical shape and separation of the keratin layer from the underlying epithelium. The length and width of filiform papillae were (551.66±29.62 & 289.63±8.99) (Fig. 2d). There were disfigured fungiform papillae with degenerated taste buds (336.22±11.29) (Fig. 2e). The circumvallate papillae had multiple degenerated taste buds (Fig. 2f). Atrophic epithelium in the ventral surface was seen (127.40±10.86) (Fig. 3d). The underlying c.t. showed severe infiltration of inflammatory cells and widening of blood vessels engorged with RBCs (783.43±22.83). There was progressive cystic degeneration (386.37±11.53) of the WG (Fig. 3e) and marked cytoplasmic vacuolization of the serous acini with obliterated ducts in VG (Fig. 3f) (Table 1). In the QRC+MTX group, there was little improvement of the lingual mucosa in comparison with the MTX group. There was a mild restoring of the conical shape of filiform papillae (797.99±13.35 & 221.92±10.45) (Fig. 2j). The width of fungiform papillae was (380.75±13.70), with degenerated taste buds (Fig. 2k). Within circumvallate papilla, there were mixed appearance of normal and degenerated taste buds (Fig. 2l). Mild increase in ventral surface thickness was evident (243.96±13.76) (Fig. 3j). The underlying c.t. showed moderate inflammation, congested blood vessels with minimal dilatation (571.35±10.85). The average cystic space was (137.74±9.52) of WG (Fig. 3k) and moderate vacuolization of serous acini in VG (Fig. 3l) (Table 1).

In the QRC-NE+MTX group, there was marked improvement of the lingual mucosa in comparison to the MTX group. Normal conical shape of filiform papillae with pointed tips was restored through measuring their length and width (1054.87±10.38&179.99±14.09) (Fig. 2m). Well-formed taste buds within both normal appearing fungiform papillae (461.81±8.69) and circumvallate papillae (Fig. 2n & 2o). The thickness of the ventral surface was within normal range (474.31±12.72) (Fig. 3m). The underlying c.t. showed

Tianjin Daxue Xuebao (Ziran Kexue yu Gongcheng Jishu Ban)/
Journal of Tianjin University Science and Technology
ISSN (Online):0493-2137
E-Publication: Online Open Access
Vol: 59 Issue: 02:2026
DOI: 10.5281/zenodo.18617972

mild inflammation with minimal dilatation of blood vessels (137.33±8.99). No cystic degeneration (67.42±5.75) within WG (Fig. 3n) and mild vacuolization of the serous acini in VG were noticed (Fig. 3o) (Table 1).

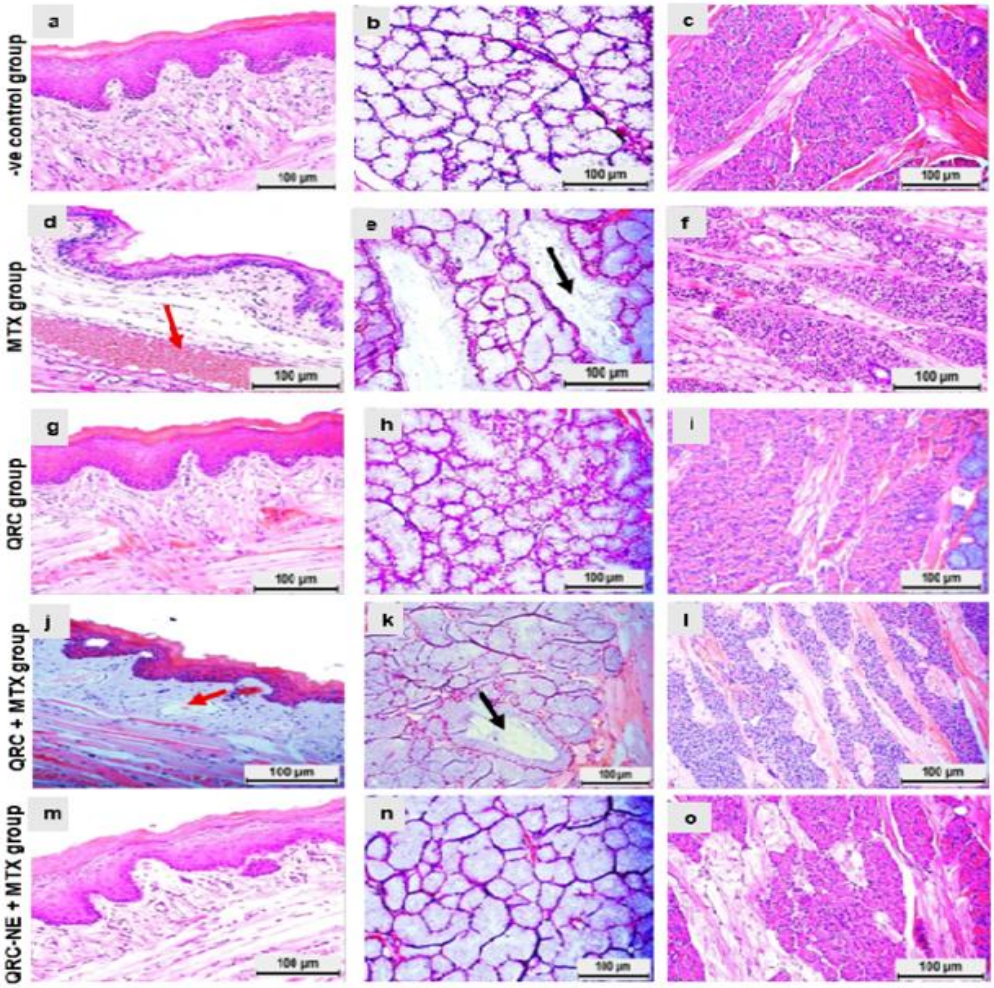

Fig. 3: Photomicrographs of lingual mucosa showing: (a-c) Negative control group (a) Normal epithelium of the ventral surface. (b)Normal microscopic picture of Weber gland. (c) Normal microscopic picture of Von Ebner gland. (d-f) MTX group (d) Atrophic epithelium with dilated blood vessel and marked inflammation. (e) Cystic transformation of mucous acini. (f) marked cytoplasmic vacuolization in the gland. (g-i) Normal histological features in QRC group. (j-l) QRC+MTX group (j) Arophic epithelium with dilated blood vessel and moderate inflammation. (k) Some cystic transformation in the mucous acini. (l) Moderate cytoplasmic vacuolization in the serous acini. (m-o) QRC-NE+MTX group (m) Normal ventral surface. (n) Normal mucous acini. (o) normal serous acini {blood vessel (red arrows), cystic formation (black arrows)} [H& E-stained sections. Magnifications: X20]

Tianjin Daxue Xuebao (Ziran Kexue yu Gongcheng Jishu Ban)/
Journal of Tianjin University Science and Technology
ISSN (Online):0493-2137
E-Publication: Online Open Access
Vol: 59 Issue: 02:2026
DOI: 10.5281/zenodo.18617972

3.4 Masson Trichrome-stained assessment:

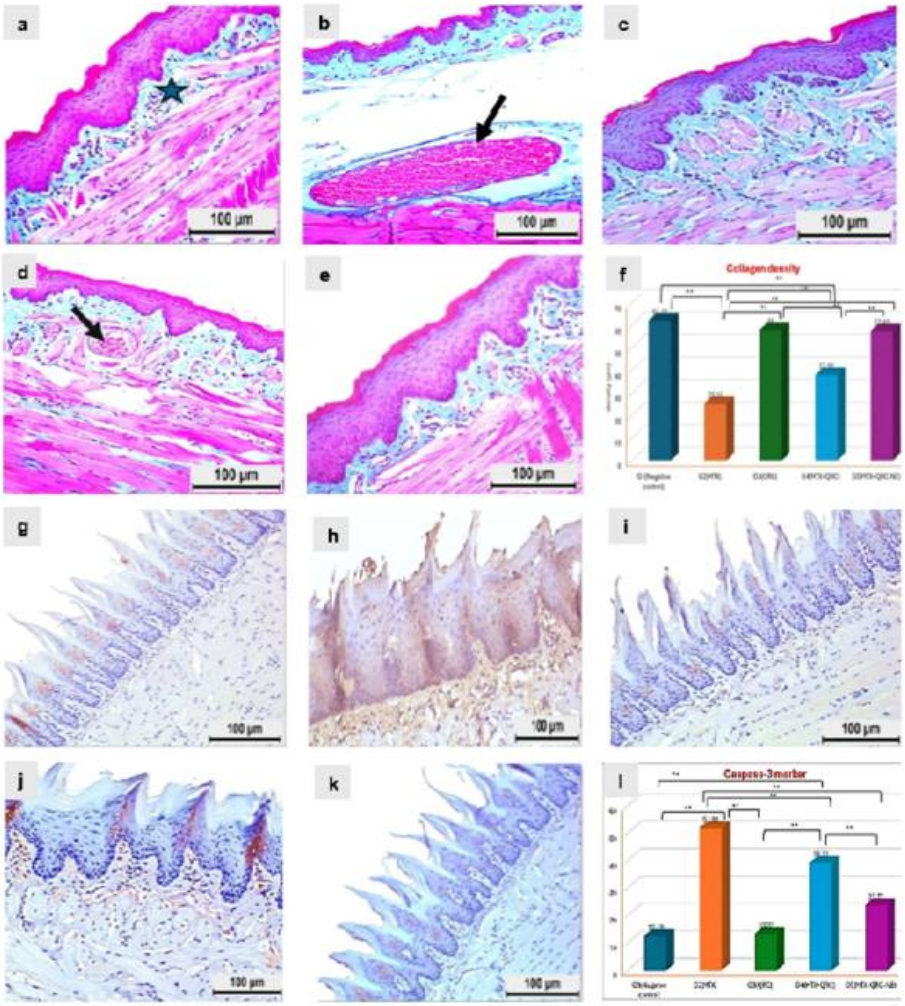

Fig. 4: (a-f) Masson Trichrome sections showing the ventral surface of the tongues (a) negative control group with normal appearance and distribution of collagen fibers in the lamina propria. (b) MTX group with loose and disorganized collagen fibers and dilated blood vessels. (c) QRC group with a normal distribution of collagen fibers. (d) QRC+MTX group with weak staining intensity of collagen fibers with a dilated blood vessel. (e) QRC-NE+MTX group with strong positive staining affinity. (f) Histogram showing the mean of collagen density and pairwise comparison between groups. {Collagen distribution (blue star), dilated blood vessels (black arrows)}. (g-l) Photomicrographs of Caspase-3 immunoexpression of lingual mucosae (g) Negative cytoplasmic reaction in the negative control group. (h) Strong expression in MTX group. (i) Mild expression in QRC group. (j) Moderate expression in QRC+MTX group. (k) Mild expression in QRC-NE+MTX group. (l) Histogram shows the mean of caspase-3 expression and pairwise comparison between the five groups. (magnifications: X20)

Tianjin Daxue Xuebao (Ziran Kexue yu Gongcheng Jishu Ban)/
Journal of Tianjin University Science and Technology
ISSN (Online):0493-2137
E-Publication: Online Open Access
Vol: 59 Issue: 02:2026
DOI: 10.5281/zenodo.18617972

Collagen fibres in the lamina propria of the negative control and QRC groups were condensed and well-organized. The mean collagen density was 62.12±5.86 and 58.00±4.64, respectively. In MTX-treated group, collagen fibres were disorganized and loose (25.16±6.06). In QRC+MTX group, the collagen fibres began to increase in its density slightly in comparison with the positive control group (37.92±4.92). While in QRC-NE+MTX group, the collagen fibres revealed more organization and density (57.43±8.11). The pairwise comparisons showed significant differences between groups, while no significant difference was detected between the negative control, QRC, and QRC-NE+MTX groups ($p<0.05$) (Fig. 4a–f) (Table 1).

3.5 Caspase-3 immunohistochemical assessment:

Negative to mild caspase-3 immunostaining was observed in the negative control and QRC groups, 12.59±0.77 & 13.32±0.97, respectively. Strong expression was observed in MTX-treated group (51.83±1.56), while moderate expression was noticed in QRC+MTX (39.21±3.24). Mild immunostaining was seen in QRC-NE+MTX (23.77±1.45). Pairwise comparison showed a significant difference between groups with no significant difference between negative control, QRC, and QRC-NE+MTX groups ($p<0.05$) (Fig. 4g–l) (Table 1).

4. DISCUSSION

Oral mucositis (OM) is one of the debilitating side effects following MTX treatment, which may worsen the patient's quality of life due to poor nutrition, pain, bleeding, and ulceration associated with it [19]. Phytochemicals are used as effective adjuvants with chemotherapies or mitigate the side effects associated with chemotherapies [20]. QRC can manage oxidative stress and inflammation-related conditions due to its antioxidant and anti-inflammatory properties [7]. To improve its low bioavailability, QRC-NE has been synthesized by the ultrasonication method, which allowed the production of a small droplet size with enhanced stability [13]. Consistent with our clinical data, weight loss is an indicator of discomfort and pain while eating. It might be attributed to diarrhoea or an acquired aversion to food that developed as a side effect of the anticancer drug [21]. Severe hair loss could be regarded to the fact that MTX targets the rapidly proliferating cells, leading to dystrophy of hair follicles [22]. The anti-inflammatory effects of QRC might partially attenuate OM induced by MTX. These findings were in accordance with **Sukhotnik *et al*. (2018),** who reported the ameliorative effect of QRC against intestinal mucositis induced by MTX [23].

Oral epithelial cells are characterized by their high metabolic activity with a higher turnover rate [19]. The degenerative changes associated with MTX in G2 could be due to the inhibition of cellular proliferation and enhancing apoptosis in rapidly dividing cells due to the deleterious damaging effect of DNA in the basal layer [24]. MTX inhibits protein synthesis and induces the production of ROS, which leads to the destruction of ductal and acinar cells [2]. The cytoplasmic vacuolization might be due to the disruption of the cytoplasmic membrane or the accumulation of lipid droplets [25]. The dilatation could be caused by an inflammatory reaction associated with MTX treatment, which elevated

Tianjin Daxue Xuebao (Ziran Kexue yu Gongcheng Jishu Ban)/
Journal of Tianjin University Science and Technology
ISSN (Online):0493-2137
E-Publication: Online Open Access
Vol: 59 Issue: 02:2026
DOI: 10.5281/zenodo.18617972

trans-endothelial permeability [26]. The decrease in collagen density might be due to inhibition of fibroblast activity that effect on collagen synthesis [27]. The expression of Caspase-3 protein increased, compared to the other groups. This could be explained by the fact that MTX induced apoptosis by either caspase activation or blocking purine and pyrimidine synthesis, leading to DNA breakdown [15].

In QRC-treated animals, the mild improvement in the histological picture of lingual mucosa could be attributed to the beneficial effects of QRC in modifying gene expression, leading to suppression of ROS production and exerting an antiapoptotic activity [28]. The potential protective role of QRC in counteracting the degenerative effects caused by MTX could be explained by the ability of QRC to promote the growth of human oral keratinocytes and improve the re-epithelialization of the oral mucosa by inhibiting oxidative stress, downregulating proinflammatory cytokines, and upregulating integrin-α6β4 expression as well as protein levels of transforming growth factor beta 3 (TGFβ3) [29]. These findings agreed with a study by **Sukhotnik *et al*. (2018),** who reported a significant decrease in the mucosal inflammation, newly formed intestinal crypts, less significant villous epithelial atrophy, and reversed intestinal mucosal damage in animals treated with MTX & QRC [23]. **Lokman *et al*. (2023)** exhibited no to mild immunopositive staining of caspase-3 in the following groups: control, QRC, and QRC (50 mg/kg) +5-FU, while moderate immunopositive staining in the QRC (25mg/kg) +5-FU group, which indicated that QRC could suppress cardiotoxicity induced by 5-FU through their potent antioxidant, antiapoptotic, and anti-inflammatory activities [30].

The marked improvement was associated with G5 (QRC-NE+MTX) resulted in improved tissue penetration and increasing the ability of collagen synthesis, with a mild cytoplasmic reaction of Caspase-3. It might be attributed to the enhancing effect of nanoparticles on the bioavailability of QRC, allowing it to counteract the inflammation, scavenging of ROS, and regulation of apoptotic signalling pathways, such as NF-κB [31]. In the present study, the dose of QRC-NE had been reduced to 12.5mg/kg in comparison with the concentration of QRC only (50 mg/kg) to avoid the toxicity induced by the nano-sized particles with a larger surface area of NE. it might be attributed to increasing the cellular uptake and changing the biological fate of bioactive components within the gastrointestinal tract (GIT) [32]. **Mahadev *et al*. (2022)** demonstrated that the formed QRC-NE, administered at a dose of 12.5 mg/kg, played a better role in controlling blood glucose levels and body weight, inhibiting oxidative stress, and reducing diabetic complications [16].

5. CONCLUSIONS

Methotrexate (MTX) has significant cytotoxic effects on the lingual mucosa, presenting a clinical challenge. Pretreatment with QRC-NE improved MTX- induced lingual mucositis compared to free QRC. Caspase-3 played a prominent role in detecting the early signs of apoptosis. These results suggest that QRC delivered in nanoemulsion form may enhance protective effects, although further mechanistic and pharmacokinetic studies are needed to confirm its efficacy.

Tianjin Daxue Xuebao (Ziran Kexue yu Gongcheng Jishu Ban)/
Journal of Tianjin University Science and Technology
ISSN (Online):0493-2137
E-Publication: Online Open Access
Vol: 59 Issue: 02:2026
DOI: 10.5281/zenodo.18617972

Acknowledgement

Declared none.

Data Availability Statement

The datasets used and/or analyzed during the current study are available from the corresponding author.

Conflict of Interest

The authors declare no conflicts of interest.

Funding

No external funding was received for this study.

Reference

1) Herfarth HH, Kappelman MD, Long MD, Isaacs KL. Use of methotrexate in the treatment of inflammatory bowel diseases. Inflamm Bowel Dis. 2016;22(1):224-233. https://doi.org/10.1097/MIB.0000000000000589

2) Taha RM, Abdel-Latif GA, Said RH. The prospective effect of green tea versus pomegranate peels extracts on submandibular salivary glands of albino rats after methotrexate administration (histological and immunohistochemical study). Int J Dent. 2024;2024:3290187. https://doi.org/10.1155/2024/3290187

3) Shao Y, Tan B, Shi J, Zhou Q. Methotrexate induces astrocyte apoptosis by disrupting folate metabolism in the mouse juvenile central nervous system. Toxicol Lett. 2019;301:146-156. https://doi.org/10.1016/j.toxlet.2018.11.016

4) Curra M, Pellicioli AC, Filho NA, Ochs G, Matte Ú, Filho MS, *et al*. Photobiomodulation reduces oral mucositis by modulating NF-kB. J Biomed Opt. 2015;20(12): 125008. https://doi.org/10.1117/1.JBO.20.12.125008

5) Raber-Durlacher JE, Elad S, Barasch A. Oral mucositis. Oral Oncol. 2010; 46(6):452-456. https://doi.org/10.1016/j.oraloncology.2010.03.012

6) Rauf A, Imran M, Khan IA, Ur-Rehman M, Gilani SA, Mehmood Z, *et al*. Anticancer potential of quercetin: A comprehensive review. Phytother Res. 2018;32(11):2109-2130. https://doi.org/10.1002/ptr.6155

7) Tang SM, Deng XT, Zhou J, Li QP, Ge XX, Miao L. Pharmacological basis and new insights of quercetin action in respect to its anti-cancer effects. Biomed Pharmacother. 2020;121:109604. https://doi.org/10.1016/j.biopha.2019.109604

8) Zhang Y, Guan R, Huang H. Anti-Allergic Effects of Quercetin and Quercetin Liposomes in RBL-2H3 Cells. Endocr Metab Immune Disord Drug Targets. 2023;23(5):692-701. http://dx.doi.org/10.2174/1871530322666220627151830

9) Liu Y, Liang Y, Yuhong J, Xin P, Han JL, Du Y, *et al*. Advances in Nanotechnology for Enhancing the Solubility and Bioavailability of Poorly Soluble Drugs. Drug Des Dev Ther. 2024; 18:1469-1495. https://doi.org/10.2147/DDDT.S447496

10) Mirza MA, Mahmood S, Hilles AR, Ali A, Khan MZ, Zaidi SAA, *et al.* Quercetin as a Therapeutic Product: Evaluation of Its Pharmacological Action and Clinical Applications-A Review. Pharmaceuticals (Basel). 2023;16(11):1631. https://doi.org/10.3390/ph16111631

11) Mustafa M, Ahmad R, Tantry IQ, Ahmad W, Siddiqui S, Alam M, *et al.* Apoptosis: A Comprehensive Overview of Signaling Pathways, Morphological Changes, and Physiological Significance and Therapeutic Implications. Cells. 2024;13(22):1838. https://doi.org/10.3390/cells13221838

Tianjin Daxue Xuebao (Ziran Kexue yu Gongcheng Jishu Ban)/
Journal of Tianjin University Science and Technology
ISSN (Online):0493-2137
E-Publication: Online Open Access
Vol: 59 Issue: 02:2026
DOI: 10.5281/zenodo.18617972

12) Fereidouni S, Kumar RR, Chadha VD, Dhawan DK. Quercetin plays protective role in oxidative induced apoptotic events during chronic chlorpyrifos exposure to rats. J Biochem Mol Toxicol. 2019;33(8): e22341. https://doi.org/10.1002/jbt.22341

13) Son HY, Lee MS, Chang E, Kim SY, Kang B, Ko H, *et al*. Formulation and Characterization of Quercetin-loaded Oil in Water Nanoemulsion and Evaluation of Hypocholesterolemic Activity in Rats. Nutrients. 2019;11(2):244. https://doi.org/10.3390/nu11020244

14) Charan J, Biswas T. How to calculate sample size for different study designs in medical research?. Indian J Psychol Med. 2013; 35(2): 121-126. https://doi.org/10.4103/0253-7176.116232

15) Yuksel Y, Yuksel R, Yagmurca M, Haltas H, Erdamar H, Toktas M, Ozcan O. Effects of quercetin on methotrexate-induced nephrotoxicity in rats. Hum Exp Toxicol. 2017;36(1):51-61. https://doi.org/10.1177/0960327116637414

16) Mahadev M, Nandini HS, Ramu R, Gowda DV, Almarhoon ZM, Al-Ghorbani M, et al. Fabrication and Evaluation of Quercetin Nanoemulsion: A Delivery System with Improved Bioavailability and Therapeutic Efficacy in Diabetes Mellitus. Pharmaceuticals (Basel). 2022;15(1):70. https://doi.org/10.3390/ph15010070

17) Patel A, Rajesh S, Chandrashekhar VM, Rathnam S, Shah K, Mallikarjuna Rao C, Nandakumar K. A rat model against chemotherapy plus radiation-induced oral mucositis. Saudi Pharm J. 2013;21(4):399-403. https://doi.org/10.1016/j.jsps.2012.11.003

18) Pu X, Storr SJ, Zhang Y, Rakha EA, Green AR, Ellis IO, and Martin S.G. (2017). 'Caspase-3 and caspase-8 expression in breast cancer: caspase-3 is associated with survival'. Apoptosis, 22(3), pp.357-368. https://doi.org/10.1007/s10495-016-1323-5

19) Ahmad A, Kazi MS. Histological Effect of Methotrexate and Folinic Acid on Oral Epithelium of Albino Rats. J Coll Physicians Surg Pak. 2016;26(6):455-458.

20) Rahman MA, Hannan MA, Dash R, Rahman MH, Islam R, Uddin MJ, *et al*. Phytochemicals as a Complement to Cancer Chemotherapy: Pharmacological Modulation of the Autophagy-Apoptosis Pathway. Front Pharmacol. 2021;12:639628. https://doi.org/10.3389/fphar.2021.639628

21) Al-Amouri FM, Badrasawi M. Taste alteration and its relationship with nutritional status among cancer patients receiving chemotherapy, cross-sectional study. PLoS One. 2024;19(5):e0302990. https://doi.org/10.1371/journal.pone.0302990

22) Medellín-Luna MF, Castañeda-Delgado JE, Fernández-Ruiz JC, Ochoa-González FL, Troncoso-Vázquez L, García-Cruz S, *et al.* Methotrexate reduces keratinocyte proliferation, migration and induces apoptosis in HaCaT keratinocytes in vitro and reduces wound closure in Skh1 mice in vivo. J Tissue Viability. 2021;30(1):51-58. https://doi.org/10.1016/j.jtv.2020.10.004

23) Sukhotnik I, Moati D, Shaoul R, Loberman B, Pollak Y, Schwartz B. Quercetin prevents small intestinal damage and enhances intestinal recovery during methotrexate-induced intestinal mucositis of rats. Food Nutr Res. 2018;62. https://doi.org/10.29219/fnr.v62.1327

24) Bilginaylar K, Aykac A, Sayiner S, Özkayalar H, Şehirli AÖ. Evaluation of the antiapoptotic and anti-inflammatory properties of chitosan in methotrexate-induced oral mucositis in rats. Mol Biol Rep. 2022;49(4):3237-3245. https://doi.org/10.1007/s11033-022-07158-x

25) Ozkorkmaz EG, Gul N, Ozluk A, Ozay Y. (2018). Ultrastructural Alterations of Liver Tissue Cells in Methotrexate-Treated Balb/c Mice. J Microsc Ultrastruct, *6*(4), 192-196.

26) Garipardic M, Bakan V, Davutoğlu M, Sayar H, Kurutaş EB. Oxidative stress and protective effect of erythropoietin on methotrexate-induced esophageal damage. J Pediatr Hematol Oncol. 2010;32(2):108-112. https://doi.org/10.1097/MPH.0b013e3181ccb678

Tianjin Daxue Xuebao (Ziran Kexue yu Gongcheng Jishu Ban)/
Journal of Tianjin University Science and Technology
ISSN (Online):0493-2137
E-Publication: Online Open Access
Vol: 59 Issue: 02:2026
DOI: 10.5281/zenodo.18617972

27) Nabai L, Kilani RT, Aminuddin F, Li Y, Ghahary, A. Methotrexate modulates the expression of MMP-1 and type 1 collagen in dermal fibroblast. Mol Cell Biochem. 2015;409(1-2):213-224. https://doi.org/10.1007/s11010-015-2526-8

28) Luangaram S, Kukongviriyapan U, Pakdeechote P, Kukongviriyapan V, Pannangpetch P. Protective effects of quercetin against phenylhydrazine-induced vascular dysfunction and oxidative stress in rats. Food Chem Toxicol. 2007;45(3):448-55. https://doi.org/10.1016/j.fct.2006.09.008

29) Hujiahemaiti M, Sun X, Zhou J, Lv H, Li X, Qi M, *et al.* Effects of quercetin on human oral keratinocytes during re-epithelialization: An in vitro study. Arch Oral Biol. 2018;95:187-194. https://doi.org/10.1016/j.archoralbio.2018.08.004

30) Lokman MS, Althagafi HA, Alharthi F, Habotta OA, Hassan AA, Elhefny MA, *et al.* Protective effect of quercetin against 5-fluorouracil-induced cardiac impairments through activating Nrf2 and inhibiting NF-κB and caspase-3 activities. Environ Sci Pollut Res Int. 2023;30(7):17657-17669. https://doi.org/10.1007/s11356-022-23314-z

31) El-Mansy MN, Hamdy ZM, Abdelsamie AE, and El-Borady OM. Synthesis of a Nano-emulsion of Quercetin Encapsulated Vitamin E Conjugated Iron Oxide Nanoparticles for the Systemic Phyto-Preventive Effect: characterization and Oral Cancer Application'. Nanoscale Advances. 2025. https://doi.org/10.1039/d5na00546a

32) McClements DJ, Rao J. Food-grade nanoemulsions: formulation, fabrication, properties, performance, biological fate, and potential toxicity. Crit Rev Food Sci Nutr. 2011;51(4):285-330. https://doi.org/10.1080/10408398.2011.559558